

Ferroelectric all-polymer hollow Bragg fibers for terahertz guidance

Maksim Skorobogatiy^{a)} and Alexandre Dupuis^{b)}

École Polytechnique de Montréal, Génie Physique, C.P. 6079, Succ. Centre-Ville, Montreal, Québec, Canada H3C3A7

(Received 12 October 2006; accepted 8 February 2007; published online 16 March 2007)

Design of hollow all-polymer Bragg fibers using periodic multilayers of ferroelectric polyvinylidene fluoride (PVDF) polymer and a low loss polycarbonate (PC) polymer is demonstrated. Efficient band gap guiding is predicted near the transverse optical frequency of a PVDF material in the terahertz regime. Optimal reflector designs are investigated in the whole terahertz region. Depending on frequency, the lowest loss hollow Bragg fiber can be one of the following: a photonic crystal fiber guiding in the band gap regime, a metamaterial fiber with a subwavelength reflector period, a single PC, or a PVDF tube. © 2007 American Institute of Physics.
[DOI: 10.1063/1.2713137]

Waveguides for the terahertz regime have recently received considerable attention due to the potential of this wavelength region for biochemical sensing, noninvasive imaging, and spectroscopy. Terahertz wavelengths cover the range of 30–3000 μm , bridging the gap between the microwave and optical regimes. One of the earliest applications of terahertz radiation was spectroscopy and chemical identification of gases.¹ It was also recognized that, due to substantial subsurface penetration of the terahertz radiation into dry dielectrics, it could be used for tomographic imaging and quality control of electronic circuits.^{2,3} Combining spectroscopic and imaging approaches resulted in propositions for nondestructive detection applications such as sensing and spatial mapping of specific organic compounds for security applications.³ Although terahertz radiation is strongly absorbed by water, biological tissue imaging has been also demonstrated.^{4,5} Finally, time resolved terahertz spectroscopy offers a noncontact way of measuring the time-dependent dielectric response of material.⁶

Development of waveguides for terahertz is motivated by the necessity of remote delivery of broad band terahertz radiation from a, generally bulky, terahertz source. The main challenge in the design of terahertz waveguides is the high absorption losses of most materials in the terahertz region. These losses hinder the development of solid core total internal reflection (TIR) fibers, while the high losses of metals hinder the development of hollow metallic guides. The earliest terahertz waveguides were metal electrodes on a semiconductor substrate⁷ exhibiting ~ 100 dB/cm transmission loss at ~ 1 THz. Later, solid core TIR waveguides such as a single mode plastic ribbon waveguide,⁸ a single crystal sapphire fiber,⁹ and a stainless steel hollow core fiber¹⁰ were demonstrated to have ~ 5 dB/cm losses at ~ 1 THz. Recently, a variety of complex low loss waveguides have been demonstrated at 1 THz. These include plastic solid core holey fibers^{11,12} (1–3 dB/cm), copper plates separated by a small air gap¹³ (0.5 dB/cm), subwavelength plastic fibers¹⁴ (0.5 dB/cm), hollow polymer waveguides with inner metallic or metalliclike layers^{15–17} (6–20 dB/m), and metal wires with plasmon mediated guidance^{18,19} (1–10 dB/m).

Theoretical work presented in this letter is motivated by the recent experimental advance of our group in the fabrica-

tion of hollow Bragg fibers featuring periodic multilayer reflectors consisting of ferroelectric polyvinylidene fluoride (PVDF) and low loss polycarbonate (PC) polymers. In one approach, we use consecutive deposition of polymer layers by solvent evaporation on the inside of a rotating polymer tube.²⁰ This results in a large core diameter of ~ 1 cm preform, which can be also considered to be a short terahertz waveguide [Fig. 1(a)]. An alternative fabrication method uses corolling and solidification of two dissimilar polymer films, also resulting in a preform [Fig. 1(b)], which may be drawn later,²¹ into a smaller diameter fiber [Fig. 1(c)]. Hidaka *et al.*,¹⁷ have demonstrated that when a layer of ferroelectric PVDF polymer is placed on the inside of a plastic tube, the resulting structure presents an efficient terahertz waveguide. Detailed analysis shows that PVDF polymer exhibits efficient metal-like reflectivity and considerably lower absorption losses, compared to those of metals in the vicinity of 1 THz. In this letter we demonstrate theoretically that hollow core Bragg fiber, featuring a periodic reflector containing ferroelectric PVDF and low loss PC polymers, may be designed to exhibit large terahertz band gaps near the transverse optical frequency of PVDF. We find that, depending on the frequency of operation, the lowest loss hollow Bragg fiber can be one of the following: a photonic crystal fiber guiding in a band gap regime, a metamaterial fiber with a subwavelength reflector period, a single PC tube of a specific

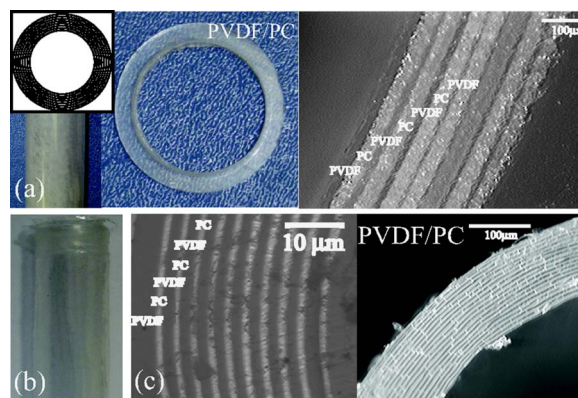


FIG. 1. (Color online) Examples of hollow all-polymer Bragg fibers. (a) Fabrication by consecutive deposition of PVDF/PC layers on the inside of a PC tube by solvent evaporation. (b) Fabrication by corolling of PVDF/PC films. (c) Smaller diameter fibers drawn from (b).

^{a)}Electronic mail: maksim.skorobogatiy@polymtl.ca

^{b)}URL: <http://www.photonics.phys.polymtl.ca>

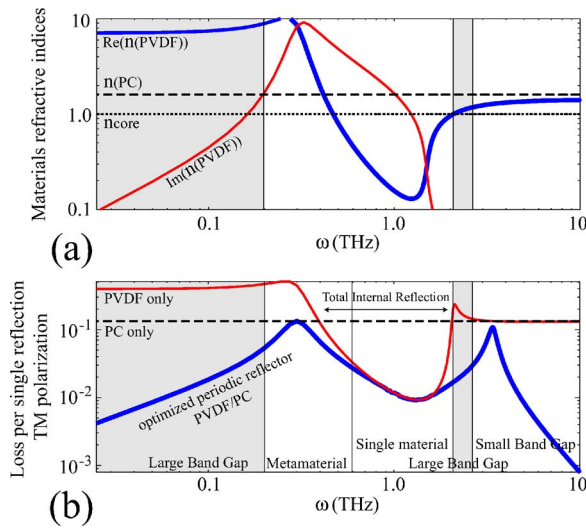


FIG. 2. (Color online) (a) Re and Im parts of the reflector material refractive indices in terahertz. (b) Reflection efficiency from the semi-infinite PC (dotted line) and PVDF (thin line) layers, as well as from an optimized reflector (thick line).

thickness, or a single PVDF tube of any thickness. In passing, we would like to note that an extra manufacturing step in fiber fabrication might be needed before fibers in Fig. 1 can be used as suggested. Particularly, PVDF polymer has to be “activated” via poling process to become ferroelectric. This can be done either during or after fiber drawing. Depending on the technique and amount of poling used, guidance in such fibers may vary. Thus, comparison of the fiber transmission data with theoretical predictions requires detailed understanding of the influence of poling conditions on the PVDF dielectric constant.

In what follows, we present a theoretical study of transmission through hollow core ferroelectric Bragg fibers (Fig. 1). Confinement in such fibers is provided by the reflector, consisting of a periodic sequence of PVDF and PC layers of thicknesses d_{PVDF} and d_{PC} , with a PVDF layer closest to the core. We assume the hollow core diameter to be significantly larger than the wavelength of the transmitted radiation. Light propagation in such fibers may be seen as a sequence of consecutive reflections, at grazing angles of incidence, from an almost planar reflector (Fig. 2, $\theta \approx 90^\circ$).

In the terahertz region, the PVDF dielectric function exhibits a resonance,

$$\epsilon_{\text{PVDF}}(\omega) = \epsilon_{\text{opt}} + \frac{(\epsilon_{\text{dc}} - \epsilon_{\text{opt}})\omega_{\text{TO}}^2}{\omega_{\text{TO}}^2 - \omega^2 + i\gamma\omega}, \quad (1)$$

where, according to Ref. 17 $\epsilon_{\text{opt}}=2.0$, $\epsilon_{\text{dc}}=50.0$, $\omega_{\text{TO}}=0.3$ THz, and $\gamma=0.1$ THz. In comparison with PVDF, the dielectric response of PC polymer is frequency independent, having a purely real dielectric constant $\epsilon_{\text{PC}}=2.56$. The material in the core is air, with $\epsilon_{\text{core}}=1.0$. In the limit when material losses are negligible and the number of reflector periods is infinite, the theory of planar periodic reflectors²² predicts that for a given angle of incidence θ onto such a reflector there exists a wavelength λ_c for which radiation of any polarization is reflected completely. Defining modal effective refractive index as $n_{\text{eff}}=n_c \sin(\theta)$, while $\tilde{n}_{\text{PVDF}}=\sqrt{n_{\text{PVDF}}^2-n_{\text{eff}}^2}$ and $\tilde{n}_{\text{PC}}=\sqrt{n_{\text{PC}}^2-n_{\text{eff}}^2}$, then $\lambda_c/2=d_{\text{PVDF}}\tilde{n}_{\text{PVDF}}+d_{\text{PC}}\tilde{n}_{\text{PC}}$. Around λ_c , there exists a wavelength range $\Delta\lambda$, called the band gap, such that, for any

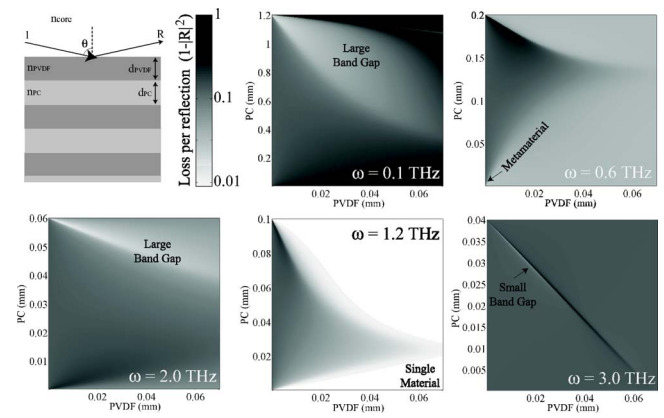


FIG. 3. Mapping of losses per single reflection from an infinite periodic reflector as a function of the layer thicknesses d_{PVDF} , d_{PC} , at various terahertz frequencies. $\theta=89^\circ$.

wavelength inside of the band gap, radiation is still completely reflected. The relative size of the band gap is proportional to the relative index contrast in the reflector multilayer $\Delta\lambda/\lambda_c \sim |\tilde{n}_{\text{PVDF}} - \tilde{n}_{\text{PC}}| / \text{average}(\tilde{n})$. Band gap size is maximized for a so-called quarter-wave reflector, where $d_{\text{PVDF}}\tilde{n}_{\text{PVDF}}=d_{\text{PC}}\tilde{n}_{\text{PC}}=\lambda_c/4$. Finally, the efficiency of a finite reflector correlates with the band gap size of a corresponding infinite reflector.

The real and imaginary parts of the refractive indices of the PVDF/PC material combination are presented in Fig. 2(a). In the regions $\omega \lesssim 0.2$ THz and $2.0 \lesssim \omega \lesssim 2.6$ THz, PVDF losses are small $\text{Im}(n) \ll \text{Re}(n)$, while the relative refractive index contrast is high suggesting the possibility of designing an efficient periodic reflector featuring a large band gap. In the region $0.6 \lesssim \omega \lesssim 2.0$ THz, the real part of the PVDF refractive index is smaller than that of air, resulting in total internal reflection from the multilayer interface. In Fig. 3 we show the loss per single reflection from the infinitely periodic reflector for the lossiest TM polarized plane wave (magnetic field parallel to the reflector interface). A grazing angle of incidence θ is fixed and equal to 89° . For every frequency, the loss is presented in shades of gray (white: low loss, black: high loss) as a function of the reflector layer thicknesses. As PC is assumed to be lossless, all the loss maps in Fig. 3 are periodic along the d_{PC} axis, where only one period is shown. For $\omega=3$ THz and higher, due to small index contrast in a multilayer, the reflector band gap is small and reflector efficiency is low. In this regime reflection from a periodic multilayer is similar to the reflection from a simple semi-infinite slab of some averaged dielectric constant. For $\omega=0.1$ THz and $\omega=2.0$ THz optimal reflectors have large band gaps, as may be seen from the extended regions of phase space ($d_{\text{PVDF}}, d_{\text{PC}}$) characterized by high reflector efficiency (white regions in the corresponding figures of Fig. 3). In the region of total internal reflection (including $\omega=1.2$ THz) we observe that reflection may be made very efficient simply by using a thick enough PVDF layer. Finally, at lower frequencies $0.2 \lesssim \omega \lesssim 0.6$ THz PVDF absorption becomes very large; to minimize reflector loss a metamaterial in the form of a reflector with subwavelength period becomes most efficient. In this configuration, reflector loss is reduced below that of PVDF due to the presence of low loss PC.

To conclude our discussion of planar reflectors, in Fig. 2(b) we compare TM reflection efficiency from the op-

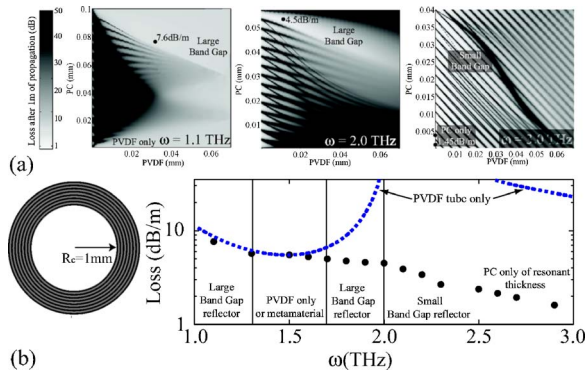


FIG. 4. (a) Mapping of the 1 mm core diameter hollow Bragg fiber transmission losses as a function of the reflector layer thicknesses at various terahertz frequencies. (b) Dots: transmission losses of the optimal hollow Bragg fiber designs. Dashed line: transmission loss of 1 mm core diameter PVDF tube guide.

timized semi-infinite periodic PVDF/PC reflector (thick curve) with the reflection efficiencies from semi-infinite slabs of PVDF (thin curve) or PC (dotted curve). For a given frequency, optimized reflector is found by first calculating a loss map (Fig. 3) of the reflector as a function of the PVDF and PC layer thicknesses, and then choosing the structure with the lowest loss. The optimal reflector guiding mechanism is indicated in Fig. 2(b) on the frequency axis. Note that reflection from a PVDF layer alone is very efficient in the frequency range of total internal reflection, when $\text{Re}(n_{\text{PVDF}}) < n_{\text{air}}$. However, beyond this region PVDF is highly absorbing and reflection from a single PC layer becomes more efficient. As periodic multilayers offer a possibility of band gap guiding and metamaterial design, it is not surprising to find from Fig. 2(b) that optimal periodic PVDF/PC reflectors dramatically outperform single material reflectors. Finally, we note that at frequencies $\omega \approx 0.3, 3.4$ THz even the optimal reflectors become inefficient for the reflection of TM polarized waves (see Ref. 22).

We conclude by presenting the theoretical transmission loss of the optimized 1 mm diameter hollow core Bragg fiber with a 31 layer PVDF/PC reflector in Fig. 4. At all frequencies, the geometry of the optimal Bragg fiber is found by first constructing fiber loss maps [Fig. 4(a)] and then choosing reflector layer thicknesses that minimize fiber transmission loss. We note that for the frequencies of ~ 1 THz, individual reflector layer thicknesses are typically ~ 50 μm . At the fiber input we assume excitation with a Gaussian beam of 0.77 mm diameter, which empirically gives the highest coupling efficiency ($\sim 90\%$ – 98%) into the HE_{11} Gaussian-like core mode of a hollow fiber. To construct fiber loss maps [Fig. 4(a)], for every choice of reflector layer thicknesses we first use the mode solver to find all the leaky and guided modes of the corresponding hollow Bragg fiber. Modal excitation coefficients are then found at the fiber input by expanding an incoming Gaussian beam into the fiber modal fields using the continuity of the transverse electromagnetic fields at the air-fiber interface. The excitation field is then propagated for 1 m. The remaining power at the fiber end is calculated, and the total loss is computed. In our simulations we find that the coupling loss is typically smaller than 0.5 dB, and the total loss of a fiber span is always dominated by the fiber loss. As discussed in the previous section, radiation propagation in the hollow core of a Bragg fiber can be

thought of as a sequence of consecutive bounces from the confining reflector. Thus, the loss of a Bragg fiber is directly determined by the efficiency of a periodic reflector. Comparing loss maps of a planar multilayer (Fig. 3) with these of a Bragg fiber [Fig. 4(a)], it is not surprising to find that at the corresponding frequencies they look very much alike. Thus, optimal design strategies for the Bragg fiber reflectors are analogous to these for the planar reflectors. For example, in the frequency region of 1.6–2.1 THz, refractive index contrast in a multilayer is high, while PVDF loss is relatively low. As a result, the optimal Bragg fiber is a band gap guiding fiber. Finally, in the 1.0–3.0 THz region we show transmission loss [dots in Fig. 4(b)] of optimally designed Bragg fibers and mark the guidance mechanisms. For comparison, we also present losses of a PVDF tube [dotted line in Fig. 4(b)] of the same bore radius and note that for frequencies higher than 1.6 THz, the optimally designed Bragg fiber considerably outperforms a PVDF tube.

To summarize, we have started with an idea that near the transverse optical frequency of a ferroelectric polymer, a tube made of such a material can be used as an efficient hollow core terahertz waveguide. We then extended this idea to introduce a hollow core Bragg fiber with a periodic reflector containing ferroelectric polymer as one of its layers. Finally, we have demonstrated that a hollow Bragg fiber with an optimally designed reflector greatly outperforms a ferroelectric tube guide. Moreover, depending on the frequency of operation optimally designed Bragg fibers may feature band gap, total internal reflection or antiresonant guiding.

- ¹R. H. Jacobsen, D. M. Mittleman, and M. C. Nuss, *Opt. Lett.* **21**, 2011 (1996).
- ²D. M. Mittleman, S. Hunsche, L. Boivin, and M. C. Nuss, *Opt. Lett.* **22**, 904 (1997).
- ³T. Kiwa, M. Tonouchi, M. Yamashita, and K. Kawase, *Opt. Lett.* **28**, 2058 (2003).
- ⁴K. Kawase, Y. Ogawa, Y. Watanabe, and H. Inoue, *Opt. Express* **11**, 2549 (2003).
- ⁵T. Lffler, T. Bauer, K. Siebert, H. Roskos, A. Fitzgerald, and S. Czasch, *Opt. Express* **9**, 616 (2001).
- ⁶M. C. Beard, G. M. Turner, J. E. Murphy, O. I. Micic, M. C. Hanna, A. J. Nozik, and C. A. Schmuttenmaer, *Nano Lett.* **3**, 1695 (2003).
- ⁷M. Y. Frankel, S. Gupta, J. A. Valdmanis, and G. A. Mourou, *IEEE Trans. Microwave Theory Tech.* **39**, 910 (1991).
- ⁸R. Mendis and D. Grischkowsky, *J. Appl. Phys.* **88**, 4449 (2000).
- ⁹S. P. Jamison, R. W. McGowan, and D. Grischkowsky, *Appl. Phys. Lett.* **76**, 1987 (2000).
- ¹⁰R. W. McGowan, G. Gallot, and D. Grischkowsky, *Opt. Lett.* **24**, 1431 (1999).
- ¹¹H. Han, H. Park, M. Cho, and J. Kim, *Appl. Phys. Lett.* **80**, 2634 (2002).
- ¹²M. Goto, A. Quema, H. Takahashi, S. Ono, and N. Sarukura, *Jpn. J. Appl. Phys., Part 1* **43**, 317 (2004).
- ¹³R. Mendis and D. Grischkowsky, *IEEE Microw. Wirel. Compon. Lett.* **11**, 444 (2001).
- ¹⁴L. J. Chen, H. W. Chen, T. F. Kao, J. Y. Lu, and C. K. Sun, *Opt. Lett.* **31**, 308 (2006).
- ¹⁵J. Harrington, R. George, P. Pedersen, and E. Mueller, *Opt. Express* **12**, 5263 (2004).
- ¹⁶T. Hidaka, *Proc. SPIE* **5135**, 11 (2003).
- ¹⁷T. Hidaka, H. Minamide, H. Ito, J. Nishizawa, K. Tamura, and S. Ichikawa, *J. Lightwave Technol.* **23**, 2469 (2005).
- ¹⁸K. L. Wang and D. M. Mittleman, *Nature (London)* **432**, 376 (2004).
- ¹⁹H. Cao and A. Nahata, *Opt. Express* **13**, 7028 (2005).
- ²⁰Y. Gao, N. Guo, B. Gauvreau, M. Rajabian, O. Skorobogata, E. Pone, O. Zabeida, L. Martinu, C. Dubois, and M. Skorobogatiy, *J. Mater. Res.* **21**, 2246 (2006).
- ²¹E. Pone, C. Dubois, N. Guo, Y. Gao, A. Dupuis, F. Boismenu, S. Lacroix, and M. Skorobogatiy, *Opt. Express* **14**, 5838 (2006).
- ²²M. Skorobogatiy, *Opt. Lett.* **30**, 2991 (2005).